Exactly soluble limit of ϕ^3 field theory with internal Potts symmetry

1979 J. Phys. A: Math. Gen. 12 689

(http://iopscience.iop.org/0305-4470/12/5/017)

J. Phys. A: Math. Gen., Vol. 12, No. 5, 1979. Printed in Great Britain

Exactly soluble limit of ϕ^3 field theory with internal Potts symmetry

D J Amit and D V I Roginsky

Racah Institute of Physics, Hebrew University, Jerusalem, Israel

Received 1 August 1978

Abstract. We consider a field theory in which the fields form a $(2l+1)$-dimensional (complex) irreducible representation of SO(3). This theory contains an additional internal discrete symmetry of the 3-state Potts model. There exists only one quadratic and one cubic invariant. There are many quartic invariants, but they are irrelevant below six dimensions as far as the infra-red behaviour is concerned. It is shown that as $l \to \infty$ the model becomes soluble. In contrast to the infinite N limit here it is the wavefunction, rather than the coupling constant, that is renormalised in a nontrivial way, as well as ϕ^2.

The asymptotic behaviour of the infinite l limit is analysed explicitly, and compared with renormalisation group results.

1. Introduction

The number of soluble interacting field theories is so small that every possible candidate deserves careful study. The importance of such models is very great, both as checks on approximations made on realistic field theories, and as a source of hypotheses on the behaviour of such theories.

A classic case in point is the infinite N limit of Landau–Ginzburg–Wilson model which was proved equivalent to the spherical model (Stanley 1971, Kac and Thompson 1971) of Berlin and Kac (1952). This soluble model has proved to be extremely fruitful in statistical physics as well as in particle physics.

The salient features of this model are an interaction of quartic type with an $O(N)$ symmetry. The fields constitute an N dimensional basis of this representation. On calculating perturbation theory one finds that graphs with different topological structures have numerical coefficients which behave as different powers of N, for large N. For the two-point function the leading graphs *at every order* are the mass insertions; for the four-point function these are the bubbles and mass insertions etc.

One chooses the coupling constant to decrease with N so that the leading graphs *at every order* have a coefficient whose asymptotic dependence on N is like that of the tree approximation. The rest of the graphs vanish in this limit. The important point is that this limit leads to a well defined nontrivial model, in contrast to such limits (which provide trivial solvability) as a vanishing charge in electrodynamics.

Coleman *et al* (1974) have tried to discredit the statement that one attains an exactly soluble model when $N \to \infty$, by comparing it with a statement that the Born approximation becomes exact as $e \to 0$ in electrodynamics. But the equivalence to the spherical model shows that the situation is very different.

0305-4470/79/050689+25$01.00

The fact that graphs with different topological structures have different powers of N stems from the fact that $O(N)$ is a continuous symmetry, though we do not know of any general statement to this effect. The permutation symmetry alone would not produce a significant discrimination between graphs. This fact has prevented the appearance of soluble versions of the Potts model (Potts 1952, Ashkin and Teller 1943).

The $(n+1)$-state Potts-model can be described by a field theory with n real components (Zia and Wallace 1975) and a Lagrangian of the form:

$$L = \tfrac{1}{2}(\nabla \boldsymbol{\phi})^2 + \tfrac{1}{2}m_0^2 \boldsymbol{\phi}^2 + (1/3!)g_{30}Q_{ijk}\phi_i\phi_j\phi_k + \ldots . \tag{1.1}$$

The ... stands for operators with more fields. The numerical tensor Q is the trilinear hypertetrahedral invariant constructed explicitly by Zia and Wallace (1975).

This model has been of considerable interest recently. Some of the applications associated with it are listed in (Amit 1976). Nevertheless there are still many puzzles associated with the theoretical study of the Potts model. To list but a few:

(i) The appearance of a fixed point in a theory whose mean-field approximation (the classical limit) predicts a discontinuous transition.

(ii) The meaning of the disappearance of the fixed point as the number of components increases or, equivalently, for a fixed number of components as the number of dimensions decreases.

(iii) Since one expands about six dimensions, how far can the ϵ expansion remain meaningful.

As all previous work on the model except (Golner 1973) has used the ϵ expansion about $d = 6$ (see e.g. Amit and Scherbakov 1974, Priest and Lubensky 1976, Amit 1976, Amit *et al* 1977), a limit-model soluble in an arbitrary number of dimensions is very desirable. This has been one of the central roles of the infinite N limit, namely, to give results beyond the ϵ expansion.

The hypertetrahedral symmetry of the cubic term in the Lagrangian (1.1) is discrete, and an increase in the number of components does not lead to any useful discrimination between graphs.

In the present article we show that this shortcoming can be circumvented in the case $n = 2$—the three-state Potts model—by superimposing a continuous symmetry on top of the discrete symmetry of three elements. The fields become a complex $(2l+1)$-dimensional irreducible representation of SO(3), and as $l \to \infty$ only graphs with simple topological structures survive. Terms beyond the cubic one are ignored since they are irrelevant for $d < 6$ (Amit 1976). The perturbation series is summed and integral equations result for the two-point function and for its temperature derivative, while the three-point function in this limit is identical to its Born approximation.

The asymptotic behaviour of the solutions of these integral equations are studied in detail and compared with results from the ϵ expansion. Apart from a description of the solvable limit we touch here only on issues (ii) and (iii) raised above. The result we find is that, while the two-point function scales everywhere in $3 < d < 6$, its temperature derivative scales only in a small part of this interval near $d = 6$.

2. Description of the model

The Landau–Ginsburg free energy density of the 3-state Potts model is:

$$L = \tfrac{1}{2}(\nabla \boldsymbol{\phi})^2 + \tfrac{1}{2}\mu^2 \boldsymbol{\phi}^2 + (1/3!)g_{30}(\phi_1{}^3 - 3\phi_1\phi_2{}^2) + (1/4!)g_{40}(\boldsymbol{\phi}^2)^2. \tag{2.1}$$

It may be rewritten in terms of a complex field

$$\psi = 2^{-1/2}(\phi_1 + i\phi_2) \qquad \boldsymbol{\phi} = (\phi_1, \phi_2) \tag{2.2}$$

as

$$L = \nabla\psi^*\nabla\psi + \mu^2\psi^*\psi + (\sqrt{2}/3!)g_{30}(\psi^3 + \psi^{*3}) + (1/3!)g_{40}(\psi^*\psi)^2 \tag{2.3}$$

where the asterisk denotes complex conjugation.

The invariance group of the model is the 6-element symmetric group S_3 (the group of permutations of three symbols), isomorphic to the crystallographic point group C_{3v} and to the dihedral group D_3. The field transformations that leave the Lagrangian (2.1) invariant are the rotations through angles $2\pi n/3$ ($n = 0, 1, 2$) in the (ϕ_1, ϕ_2) plane and the reflections $\phi_2 \to -\phi_2$. In terms of ψ the invariance group is represented by the linear transformations

$$\psi \to \psi \exp(i2\pi n/3) \qquad n = 0, 1, 2 \tag{2.4a}$$

and the antilinear ones

$$\psi \to \psi^* \exp(i2\pi n/3) \qquad n = 0, 1, 2. \tag{2.4b}$$

We define an extended multicomponent version of this model, which will still be invariant under the transformations (2.4) of each component of the field. Namely, the field has $N(=2l+1)$ complex components ψ_m, and L will be invariant under:

$$\psi_m \to \psi_m \exp(i2\pi n/3) \qquad \psi_m \to \psi_m^* \exp(i2\pi n/3)$$
$$n = 0, 1, 2 \qquad m = -l, -l+1, \ldots, l \ldots. \tag{2.5}$$

When passing to a multicomponent model, it is natural to extend the invariance group of the model in a way which (1) conserves in the best way the properties of the original model and (2) simplifies the problem. We choose the invariance group of the extended model to be:

$$S_3 \times SU(2) \approx C_{3v} \times SU(2) \approx D_3 \times SU(2). \tag{2.6}$$

The field $\{\psi_m\}$ is transformed under the N dimensional irreducible representation of SU(2). That is:

$$\psi_m \to \psi_{m'} D^{(l)m'}{}_m(u) \qquad u \in SU(2). \tag{2.7}$$

This choice of the symmetry group ensures the existence of a unique trilinear invariant for any even l, which is

$$\begin{pmatrix} m_1 & m_2 & m_3 \\ l & l & l \end{pmatrix} \psi_{m_1}\psi_{m_2}\psi_{m_3} + \text{HC} \tag{2.8}$$

and none for odd values of l. The coefficients are the $3j$-symbols (Wigner coefficients.) This is the highest relevant operator for $d < 6$. (For an odd value of l the $3j$-symbol would have been antisymmetric in its indices and the invariant (2.8) would have vanished). Here l is chosen to be even and the $3j$-symbol is thus symmetric in m_1, m_2, m_3.

The Lagrangian of the extended model is:

$$L = \nabla\bar{\psi}^m \nabla\psi_m + \mu^2\bar{\psi}^m\psi_m + (\sqrt{2}/3!)g_{30}\begin{pmatrix} m_1 & m_2 & m_3 \\ l & l & l \end{pmatrix}(\psi_{m_1}\psi_{m_2}\psi_{m_3} + \bar{\psi}^{m_1}\bar{\psi}^{m_2}\bar{\psi}^{m_3}) \\ + (1/3!)\sum_{j=0}^{2l} g_{40}^{(j)}\begin{pmatrix} m_1 & l & j \\ l & m_2 & m \end{pmatrix}\begin{pmatrix} m_3 & l & m \\ l & m_4 & j \end{pmatrix}\psi_{m_1}\bar{\psi}^{m_2}\psi_{m_3}\bar{\psi}^{m_4}. \tag{2.9}$$

Equation (2.3) is the $l = 0$ case of equation (2.9) if $g_{40}^{(0)} \equiv g_{40}$. We use real Wigner coefficients with upper and lower indices. The raising and lowering of indices is defined via:

$$A^m \equiv (-1)^{l+m}A_{-m} \qquad A_m \equiv (-1)^{l-m_A-m} \tag{2.10}$$

for any index m. Summation over doubly repeated indices is implied. Instead of writing the complex conjugate of the fields as in equation (2.3), we use in (2.9) a notation $\bar{\psi}^m$ in order to make the invariance of the various terms explicit. One should recall, however, that:

$$\bar{\psi}^m = (\psi_m)^*. \tag{2.11}$$

Finally, for even l there is an identity

$$\begin{pmatrix} m_1 & m_2 & m_3 \\ l & l & l \end{pmatrix} \equiv \begin{pmatrix} l & l & l \\ m_1 & m_2 & m_3 \end{pmatrix}. \tag{2.12}$$

The modification of the Lagrangian from (2.3) to (2.9) is analogous to giving isospin l to the 'particle' described by the field ψ; we will call the index m 'isospin index' for the sake of brevity.

We consider the Lagrangian (2.9) with $g_{40}^{(j)} = 0$. This is justified by the observation that if a critical point exists for $d < 6$ the infrared behaviour will be dominated by the trilinear term. The quadrilinear one will be irrelevant. It is convenient to introduce

$$g_0 = (\sqrt{2}/\sqrt{N})g_{30} \tag{2.13}$$

which will be held finite in the large N limit—the simplifying limit of our model. This will be shown to lead to correlation functions and free energy (the sum of vacuum graphs) which depend on N like their Born terms as is needed. The free energy becomes proportional to N and the two-point function independent of N in the large N limit.

The Lagrangian of the model is finally

$$L = \nabla\bar{\psi}^m\nabla\psi_m + \mu^2\bar{\psi}^m\psi_m \\ + (g_0/3!)\sqrt{N}\begin{pmatrix} m_1 & m_2 & m_3 \\ l & l & l \end{pmatrix}(\psi_{m_1}\psi_{m_2}\psi_{m_3} + \bar{\psi}^{m_1}\bar{\psi}^{m_2}\bar{\psi}^{m_3}). \tag{2.14}$$

3. Considerations concerning the graph expansion

The bare propagator and vertex part

$$G_{(0)m_2}^{m_1}(p) = \delta_{m_2}^{m_1}(p^2 + \mu^2)^{-1} \tag{3.1}$$

$$\Gamma_{(0)m_1m_2m_3}^{(3)} \equiv \Gamma_{(0)}^{(3)m_1m_2m_3} = (1/3!)g_0\sqrt{N}\begin{pmatrix} l & l & l \\ m_1 & m_2 & m_3 \end{pmatrix} \tag{3.2}$$

are the products of 'isoscalar' and 'isospin' factors, which suggest the application of separate graphical techniques for the spatial and 'isospin' coordinates.

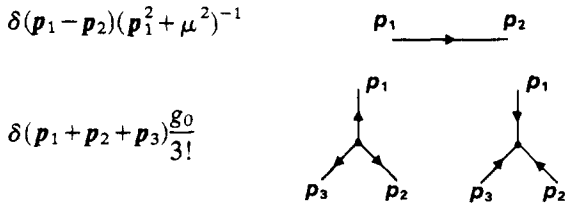

Figure 1. Propagators and vertices for the construction of the spatial part of graphs. The arrows distinguish ψ from $\bar{\psi}$.

It turns out to be convenient not to insert the $\sqrt{N}$ coefficient of equation (3.2) into the graphical notations but to multiply the contribution of a Feynman graph by $N^{n/2}$ in the nth order of perturbation theory.

Figure 2 comprises the basic notation of the angular momentum graphical technique of Levinson (1957) as extended by Jucys *et al* (1960) and by Jucys and Bandzaitis (1965)†. The notations of figure 2 differ slightly from those generally used because we confine ourself to even values of l. The signs used to denote the orientation of a node (the order of indices of the Wigner coefficients) are omitted. Note also that only external 'isospin' lines must have arrows because

$$A_m B^m \equiv A^m B_m \tag{3.3}$$

if l is even.

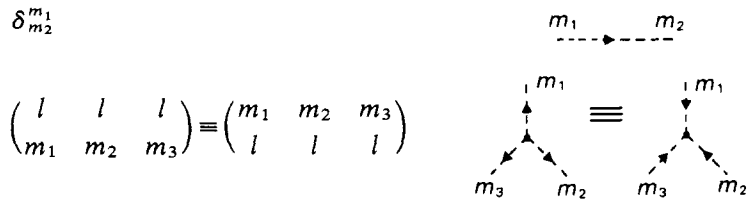

Figure 2. Propagators and vertices for the isospin part of graphs. The arrows distinguish between upper and lower indices.

According to the notation of figures 1 and 2 the propagator (3.1) is represented by the pair of lines. We will alternatively use a wavy line to represent the pair as in figure 3.

Figure 3. The combined space and isospin propagator.

Since $\phi^2 (\equiv \psi^m \psi_m)$ is an 'isoscalar', an insertion of ϕ^2 changes the 'spatial' propagator only, as is shown in figure 4.

† Similar graphical methods were introduced by Edmonds (1957) and Judd (1963); a 'dual' of Levinson graphical algorithms are those of Fano and Racah (1959); another version of the graphical techniques is used by Ponzano and Regge (1968).

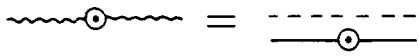

Figure 4. The ϕ^2 insertion.

The contribution of a Feynman graph to a vertex function

$$\Gamma^{(E,M)}_{(l)m_1,\ldots,m_E}(\{p_i\};\{k_j\})$$

(M is the number of ϕ^2 insertions) is a product of

(1) the 'isospin zero' Feynman graph $\Gamma^{(E,M)}_{(0)}(\{p_i\};\{k_j\})$ of the Lagrangian (2.3) with $g_{40}=0$, $\sqrt{2}g_{30}=g_0$ (this factor is independent of N) and two N dependent, but momentum independent, factors:

(2) the 'isospin' angular momentum graph $A^{(E)}_{(l)m_1,\ldots,m_E}$ (independent of M) and

(3) the overall coefficient $N^{n/2}$ for the nth order of perturbation theory.

Both graphs—the spatial one and the isospin one—are topologically identical, if one disregards the ϕ^2 insertions.

4. The isospin structure of $\Gamma^{(2)}$ and $\Gamma^{(3)}$

The relevant vertex functions of the model are those with $(E, M) = (0, 0)$, $(0, 2)$, $(2, 0)$, $(2, 1)$ and $(3, 0)$. These are primitively ultraviolet divergent. The 'isospin' graph is a closed graph when $E = 0$; it is reduced to a closed 'isoscalar' graph when $E = 2$ or 3 due to the identities depicted in figure 5 and their generalisations (figure 6).

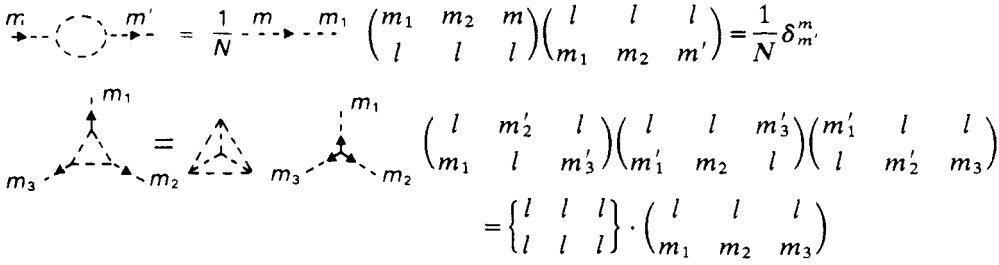

Figure 5. The basic identities of the angular momentum 'isospin' graphical technique. The tetrahedron represents the Racah–Wigner $6j$-symbol.

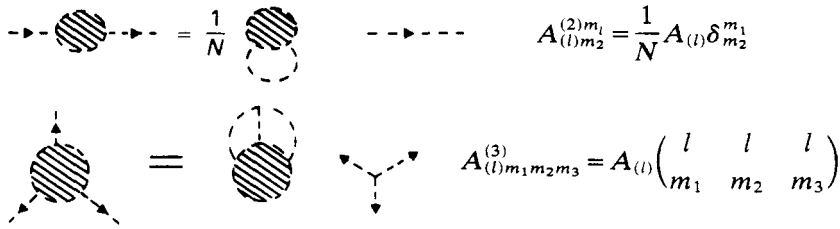

Figure 6. The identities which make the isospin structure of $\Gamma^{(2)}$ and $\Gamma^{(3)}$ explicit (Jucys 1960, equations (13.10, 13.8)).

It is therefore sufficient to consider only closed angular momentum graphs, that is the isoscalar ones. Such a graph represents a $3nj$-coefficient if it contains $2n$ nodes and (thus) $3n$ vertices.

If a closed angular momenta graph is two- or three-particle irreducible it is identical to the product of two simpler graphs as is shown graphically in figure 7 (see Jucys *et al* 1960, equations (14.5), (14.8)).

A three-particle irreducible graph is a nontrivial $3nj$-coefficient. (Generally only these ones are called $3nj$-symbols while others are called j-coefficients).

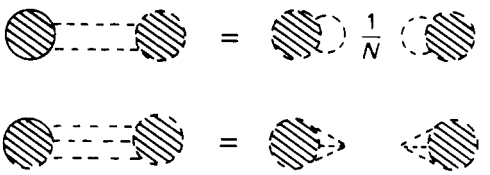

Figure 7. Factorisation of 2- and 3- particle reducible isospin graphs.

5. Large N limit—general properties of the model

Consider a closed 2PR isospin graph. It can be reduced to two simpler graphs with the help of figure 7. Suppose that any of the two graphs obtained by this reduction is either the trivial 2PI graph (figure 8) or itself 2PR, and admits a similar reduction. If no 2PI graphs arise in such successive reductions except for the trivial one (figure 8) we call the graph 'fully 2PR'.

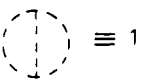

Figure 8. The simplest 2PI closed 'isospin' graph.

The second identity in figure 7 (together with figure 8) implies that such a fully 2PR $3nj$-coefficient (the most trivial nonvanishing one) is equal to

$$N^{-n+1} \tag{5.1}$$

Any other closed graph with $2n$ nodes is either a conventional (irreducible) $3nj$-coefficient or a product of the type:

$$N^{-n_0}\,.\,(3n_1j)\,.\,(3n_2j)\ldots(3n_kj) \qquad n=n_0+n_1+\ldots+n_k-k+1 \tag{5.2}$$

where $(3n_ij)$ stands for the $(3n_ij)$-coefficient.

In the large l limit the conventional $3nj$-coefficients ($n\geqslant 2$) can be shown to be asymptotically negligible compared with the fully 2PR ones. That is

$$|(3nj)|\ll N^{-n+1-\alpha} \qquad \alpha>0 \qquad N(\text{or } l)\to\infty. \tag{5.3}$$

For simple types of general $3nj$-coefficients this statement can be proved. We could not find a general proof of this asymptotic inequality, but the arguments, presented in Appendix I, together with numerical computations of the coefficients up to the $24j$, convince us that the statement is generally true, and that $\alpha\geqslant\frac{1}{2}$. Hence, any graph which is not fully 2PR contributes less than

$$N^{-n_0-n_1-\ldots-n_k+k-\alpha}=N^{-n+1-\alpha} \qquad \alpha\equiv\alpha_1+\ldots+\alpha_k>0, \qquad n\geqslant 2 \tag{5.4}$$

and is thus asymptotically negligible.

In the large N limit only those of the Feynman graphs, whose isospin closed graphs are fully 2PR, contribue to $\Gamma^{(0)}$, $\Gamma^{(0,2)}$, $\Gamma^{(2)}$, $\Gamma^{(2,1)}$ and $\Gamma^{(3)}$.

5.1. The free energy

In the kth order of perturbation theory ($k=2n$) the N-dependence of the vacuum to vacuum vertex function $\Gamma^{(0,0)}$, given by the overall power of N multiplied by (5.1) is

$$N^{k/2}\cdot N^{-n+1}=N \tag{5.5}$$

as it should. (See § 3 for the overall factor). The same is true for the energy–energy correlation function $\Gamma^{(0,2)}$ as well.

5.2. The three-point vertex

Figure 6 (the second identity) implies that

$$\Gamma^{(3)}_{(l)m_1m_2m_3}=\begin{pmatrix} l & l & l \\ m_1 & m_2 & m_3\end{pmatrix}\Gamma^{(3)}(p,N). \tag{5.6}$$

The isoscalar function $\Gamma^{(3)}(p,N)$ in the kth order of perturbation theory is given by a closed angular momentum graph $A^{(3)}(N)$ times $N^{k/2}$ times an 'isospin zero' graph. Since the original graph of $\Gamma^{(3)}$ is 1PI, the reduced closed graph $A^{(3)}(N)$ is 2PI in any order k except for the first order.

Thus in the large N limit the isospin dependent factor of $\Gamma^{(3)}(p,N)$ in the kth order is

$$N^{k/2}A^{(3)}(N)=N^{n-1/2}N^{-n+1-\alpha}\equiv N^{1/2-\alpha}\qquad k\equiv 2n-1\geq 3 \tag{5.7}$$

while in the first order it is equal to $N^{1/2}$, as is seen from equation (3.2).

For example, in 3rd order the isospin graph is that given in figure 5. The $6j$-symbol is asymptotically of the order of equation (5.3) with $n=2$, $\alpha=\frac{1}{2}$

$$\begin{pmatrix} l & l & l \\ l & l & l\end{pmatrix}\sim N^{-3/2} \tag{5.8}$$

(Wigner 1959). Multiplying by the explicit power of N, $N^{3/2}$, appropriate to 3rd order, one finds that $\Gamma^{(3)}(p,N)$ at this order is proportional to N^0. Hence, all the corrections to the 1PI vertex part are negligible when $N\to\infty$, and the exact $\Gamma^{(3)}_{(l)}$ is

$$\Gamma^{(3)}_{(l)m_1m_2m_3}=(g_0/3!)\sqrt{N}\begin{pmatrix} l & l & l \\ m_1 & m_2 & m_3\end{pmatrix}, \tag{5.9}$$

which is just the Born term—equations (3.2) or (2.14).

Furthermore, since asymptotically

$$\begin{pmatrix} l & l & l \\ m_1 & m_2 & m_3\end{pmatrix}\simeq N^{-1/2}; \tag{5.10}$$

(Ponzano and Regge 1968), the components of $\Gamma^{(3)}_{(l)m_1m_2m_3}$ have finite limits as $N\to\infty$.

5.3. The two-point function

Figure 6 implies that

$$\Gamma^{(2)m_1}_{(l)m_2}=\delta^{m_1}_{m_2}\Gamma^{(2)}(p,N)\qquad \Sigma^{m_1}_{(l)m_2}=\delta^{m_1}_{m_2}\Sigma(p,N) \tag{5.11}$$

The leading contribution in the large N limit is again given by the fully 2PR graphs and the isospin factor of both $\Gamma^{(2)}(p, N)$ and $\Sigma(p, N)$ in the kth order of perturbation theory ($k = 2n$) is

$$N^{k/2}N^{-1}N^{-n+1} = 1 \tag{5.12}$$

(which reproduces again the N dependence of the Born term), so that the large N limits

$$\lim_{N\to\infty} \Gamma^{(2)}(p, N) \equiv \Gamma(p) \qquad \lim_{N\to\infty} \Sigma(p, N) \equiv \Sigma(p) \tag{5.13}$$

are finite.

The function $\Gamma(p)$ and $\Sigma(p)$ are connected by the Dyson equation

$$\Gamma(p) = p^2 + \Delta\mu^2 - [\Sigma(p) - \Sigma(0)] \qquad \Delta\mu^2 = \mu^2 - \mu_c^2 \tag{5.14}$$

μ_c^2 is the relative critical temperature. Recalling that the 3-point vertex in the large N limit is given by its Born term, we arrive at a $\Sigma(p)$, which is the sum of the set of graphs in figure 9, and which can be translated to the language of skeleton graphs as is shown in figure 10. Figure 10 is simply the statement that all graphs in figure 9 are propagator corrections to the first one.

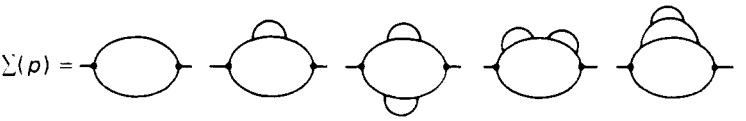

Figure 9. Graphs contributing to the self-energy in the large N limit.

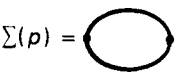

Figure 10. The self-energy in terms of skeleton graphs. The thick line represents the full Green function.

Thus the Dyson equation of the model is a closed integral equation for $G(p)$:

$$G^{-1}(\boldsymbol{p}) = p^2 + \Delta\mu^2 - \frac{g_0^2}{2}\int_{|\boldsymbol{q}|<\Lambda} \frac{\mathrm{d}^d q}{(2\pi)^d} G(\boldsymbol{q})[G(\boldsymbol{p}+\boldsymbol{q}) - G(\boldsymbol{q})]. \tag{5.15}$$

This should be compared with equations such as those of Patashinski and Pokrovski (1964). Note that there the equation is an arbitrary approximation to the skeleton series while here it is a well defined limit of the model.

5.4. The vertex with ϕ^2 insertion

The ϕ^2 insertion is the insertion of a 'isospin' invariant $\bar{\psi}^m\psi_m$ and, consulting figure 6, one has:

$$\Gamma^{(2,1)m_1}_{(l)m_2} = \delta^{m_1}_{m_2}\Gamma^{(2,1)}(\boldsymbol{p}_1, \boldsymbol{p}_2) \tag{5.16}$$

with $\Gamma^{(2,1)}(\boldsymbol{p}_1, \boldsymbol{p}_2)$ independent of N in the large N limit. $\Gamma^{(2,1)}(\boldsymbol{p}_1, \boldsymbol{p}_2)$ is the sum of those graphs of the 'isospinless' model, whose isospin counterparts become fully 2PR closed graphs after the reduction with the help of figure 6. The difference from the case of $\Gamma^{(2,0)}$ is that although the ϕ^2 insertion does not change the isospin graph, corresponding to a

given 'isospinless' graph, it changes the set of the contributing graphs of the latter kind. Written in terms of skeleton graphs, to avoid listing all the propagator corrections, the contributions to $\Gamma^{(2,1)}$ as $N \to \infty$ are those shown in figure 11. It follows from figure 11 that $\Gamma^{(2,1)}$ satisfies a linear integral equation

$$\Gamma^{(2,1)}(\boldsymbol{p}_1, \boldsymbol{p}_2) = 1 + g_0^2 \int \frac{\mathrm{d}^d q}{(2\pi)^d} \Gamma^{(2,1)}(\boldsymbol{p}_1 - \boldsymbol{q}, \boldsymbol{p}_2 + \boldsymbol{q}) G(\boldsymbol{q}) G(\boldsymbol{p}_1 - \boldsymbol{q}) G(\boldsymbol{p}_2 + \boldsymbol{q}) \tag{5.17}$$

which together with (5.15) determines both functions. The special case of equation (5.17) when the momentum of the ϕ^2 is zero (that is $\boldsymbol{p}_2 = -\boldsymbol{p}_1$) can be derived from equation (5.15) utilising the relation

$$\Gamma^{(2,1)}(\boldsymbol{p}, -\boldsymbol{p}) = \frac{\partial}{\partial \mu^2} \Gamma^{(2)}(p) \tag{5.18}$$

which means that the insertion of a ϕ^2 at zero momentum is equivalent to a derivative with respect to the temperature. This special case of the $\Gamma^{(2,1)}$ equation will be analysed in § 8.

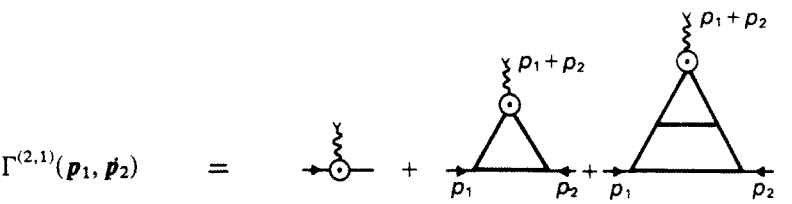

Figure 11. The series of skeleton graphs contributing to $\Gamma^{(2,1)}$ as $N \to \infty$. The thick lines are full propagators, and ⊙ denotes the insertion of ϕ^2.

6. The correlation function at the critical point

We study the system at its critical (massless) point. The parameters of the theory are chosen to be:

$$\Delta\mu^2 = 0 \tag{6.1}$$

$$g_0 = u_0 \Lambda^{\epsilon/2} \equiv w_0 S_d^{-1/2} \Lambda^{\epsilon/2} \tag{6.2}$$

$$\epsilon = 6 - d. \tag{6.3}$$

The angular factor

$$S_d = [2^{d-1} \pi^{d/2} \Gamma(d/2)]^{-1} \tag{6.4}$$

is absorbed into the coupling constant w_0, and in all momentum integrals this factor will be omitted. The equation for the two-point function will take on the form:

$$G^{-1}(p) = p^2 - \tfrac{1}{2} w_0^2 \Lambda^{\epsilon} \int^{\Lambda} \mathrm{d}^d q G(q)[G(\boldsymbol{p} + \boldsymbol{q}) - G(q)]. \tag{6.5}$$

Assuming that G behaves asymptotically as

$$G(p) \sim h \Lambda^{-\eta} p^{\eta - 2} \tag{6.6}$$

when $p \ll \Lambda$, one finds for the integral on the r.h.s. of equation (6.5)

$$f(p, \Lambda) = \int^{\Lambda} d^d q q^{\eta-2}(|\boldsymbol{p}+\boldsymbol{q}|^{\eta-2} - q^{\eta-2}). \tag{6.7}$$

This integral is convergent in the ultraviolet and well-defined in the infra-red, if

$$(\epsilon/2) - 1 < \eta < (\epsilon/2). \tag{6.8}$$

We suppose that these inequalities hold, and show *a posteriori* that they indeed do.

The leading term in f for Λ large, can then be computed by dimensional regularisation ('t Hooft and Veltman 1972, Amit 1978). The result is

$$\lim_{\Lambda\to\infty} f(p, \Lambda) = -C(d, \eta) p^{2-\epsilon+2\eta} \tag{6.9}$$

with:

$$C(d, \eta) = -\tfrac{1}{2}\Gamma(\tfrac{1}{2}d)\Gamma(2-\eta-\tfrac{1}{2}d)\Gamma^2(\tfrac{1}{2}d-1+\tfrac{1}{2}\eta)/[\Gamma(d-2+\eta)\Gamma^2(1-\tfrac{1}{2}\eta)]. \tag{6.10}$$

Because of equation (6.8) the integral term dominates the p^2 in equation (6.5) for small p and one can find $\eta(d)$ for which G of equation (6.6) satisfies (6.5) in the limit $p \to 0$. The result is $\eta = \epsilon/3$, exactly.

There is, of course, a transient, in the sense of Wilson (1972) given by the p^2 terms relative to $p^{2-\eta}$. But, for any ϵ there is a characteristic value of p, p_0, such that the infra-red behaviour is attained for $p \ll p_0$. The value of p_0 shrinks to zero if η is small (when $\epsilon \to 0$, for example)—the transient is slow. This slow transient can be eliminated (Wilson 1972) by a special choice of w_0—the fixed point.

This again can be studied explicitly. To calculate the corrections to (6.9) in powers of p/Λ) one rewrites f of (6.7) as:

$$f(p, \Lambda) = \int_0^p dq q^{d-5+2\eta}(q/p)^{1-b} F(a, b; c; q^2/p^2)$$
$$+ \int_p^{\Lambda} dq q^{d-5+2\eta} F(a, b; c; p^2/q^2) - \int_0^{\Lambda} dq q^{d-5+2\eta} \tag{6.11}$$

after performing the angular integration and removing a factor of S_d, which was absorbed into the coupling constant. a, b and c are given by:

$$a = 1 - \tfrac{1}{2}\eta \qquad b = 2 - \tfrac{1}{2}(d+\eta) \qquad c = \tfrac{1}{2}d.$$

The first term in (6.11) is independent of Λ. Hence:

$$\frac{\partial f}{\partial \Lambda} = \Lambda^{d-5+2\eta}[F(a, b; c; p^2/\Lambda^2) - 1] \underset{\Lambda\to\infty}{\sim} (2\eta - \epsilon) E p^2 \Lambda^{-\epsilon-1+2\eta}[1 + O(p^2/\Lambda^2)] \tag{6.12}$$

with

$$E = (2-\eta)(4-d-\eta)/2d(2\eta-\epsilon). \tag{6.13}$$

The two leading terms in f are

$$f(p, \Lambda) = [-Cp^{2-\epsilon+2\eta} + E\Lambda^{2\eta-\epsilon}p^2][1 + O(p^2/\Lambda^2)]. \tag{6.14}$$

Inserting f back in the integral equation (6.5) the slow transient—the second term in (6.12)—can be exactly cancelled against the p^2, if w_0 and h are appropriately chosen. Equation (6.5) is then satisfied up to corrections of $O(p^2/\Lambda^2)$.

The proper choice is:

$$\eta = \epsilon/3 \tag{6.15}$$

$$w_0^{*2} = 2C^{*2}E^{*-3} \tag{6.16}$$

$$h = C^{*-1}E^{*} \tag{6.17}$$

where

$$C^{*} = -\frac{1}{2}\frac{\Gamma(d/2)\Gamma(-d/6)\Gamma^2(d/3)}{\Gamma(2d/3)\Gamma^2(d/6)} \tag{6.18}$$

$$E^{*} = (d-3)/3(6-d) \tag{6.19}$$

are the values of C and E ((6.10), (6.13)) at $\eta = \epsilon/3$. Note that this value of η satisfies the inequality (6.8).

So far ϵ was used only as a convenient notation, not as an approximation. If the expressions are expanded about $\epsilon = 0$ one finds:

$$w_0^{*2} = 2\epsilon.$$

This value coincides with the value of the fixed point found previously for the three-state Potts model (Amit 1976) in first order in ϵ. To make the comparison transparent one has to note that (1) at order ϵ the renormalised and bare coupling constant are equal and (2) that the definitions of the coupling constant in equation (2.1) above and equation (2.1) of Amit (1976) are different: $w_0^2 = 9u_0^2$, where u_0 is the dimensionless coupling constant of Amit (1976).

Finally, equations (6.16) and (6.17) indicate that

$$d = \epsilon = 3$$

is a natural boundary, at which w_0^{*2} runs away and then changes sign.

7. The correlation function in the renormalisation group approach

In the renormalisation group approach one computes the renormalisation constants, which render the theory finite at six dimensions, from them one obtains the Gell-Man–Low–Wilson functions, and finally the critical behaviour.

In the present model, in the large N limit, the renormalisation of the coupling constant is trivial, because only the Born term contributes to $\Gamma^{(3)}$. Thus the relation between the bare coupling constant g_0 and the renormalised one g is simply:

$$g_0 = Z_\phi^{-3/2} g \tag{7.1}$$

where Z_ϕ is the field renormalisation constant.

If κ is the momentum scale which enters when the theory is renormalised at zero external momentum (Brezin *et al* 1976, Amit 1976) then we can write:

$$u = \kappa^{-\epsilon/2} g = \kappa^{-\epsilon/2} Z_\phi^{3/2} g_0. \tag{7.2}$$

The function β, which determines the flow of the renormalised coupling constant, is defined by:

$$\beta(u) = \kappa \frac{\partial}{\partial \kappa} u$$

with g_0 and Λ kept fixed. In our case:

$$\beta(u) = \tfrac{1}{2}\epsilon u + \tfrac{3}{2}u\eta(u) \tag{7.3}$$

where

$$\eta(u) = \frac{\partial}{\partial \kappa} \ln Z_\phi|_{g_0,\Lambda} \tag{7.4}$$

is the anomalous dimension function of the field.

If $\beta(u^*) = 0$, then $\eta(u^*) = \eta$—the critical exponent associated with the correlations function discussed in the previous section. But equations (7.3) and (7.4) imply directly that if a nontrivial fixed point ($u^* \neq 0$) exists, then

$$\eta(u^*) = \epsilon/3. \tag{7.5}$$

8. The ϕ^2-insertion, critical behaviour in temperature

To discuss the exponent ν—the anomalous dimension of the ϕ^2 operator—we consider the function $\Gamma^{(2,1)}$. The inserted operator was defined in § 5 as

$$\phi^2 \equiv \bar{\psi}^m \psi_m.$$

The equation satisfied by $\Gamma^{(2,1)}$ was derived in § 5, equation (5.17).

We consider the massless theory at the special value of the coupling constant, given by equation (6.16). It should be remembered that the slow transients have been eliminated by this special choice of w_0. Next we choose the special case in which the momentum of the ϕ^2 is equal to zero, as was mentioned at the end of § 5. In this case equation (5.17) assumes the form

$$\psi(p) = 1 + w_0^{*2} \Lambda^\epsilon \int_{0<q<\Lambda} \mathrm{d}^d q \psi(q) G^2(\boldsymbol{q}) G(\boldsymbol{p}-\boldsymbol{q}) \tag{8.1}$$

where

$$\psi(p) \equiv \Gamma^{(2,1)}(\boldsymbol{p}, -\boldsymbol{p}). \tag{8.2}$$

Considering equation (8.1) at small momenta ($p \ll \Lambda$) we substitute in it the Green function G in its scaling form (6.6). The difference between the new integral in the equation, following the substitution, and the original one is a finite constant in the small momentum limit. This follows simply from the two observations:

(a) the integral term of (8.1) is dimensionless and

(b) $\psi(q)$ and $G(q)$ are nonsingular at finite values of q. Thus, equation (8.1) can be rewritten, at small p, as

$$\psi(p) = Q_0 + 2C^{*-1} \int_{0<q<\Lambda} \mathrm{d}^d q \frac{\psi(q)}{(\boldsymbol{q}^2)^{d/3}[(\boldsymbol{p}-\boldsymbol{q})^2]^{d/6}} \tag{8.3}$$

where C^* is given by (6.18) and Q_0 is a constant. Note that $C^* > 0$ for $0 < \epsilon < 6$. For small values of ϵ

$$C^{*-1} \approx \epsilon. \tag{8.4}$$

To fix the notation we recall that if $\Gamma^{(N,M)}$ is scale invariant it obeys:

$$\Gamma^{(N,M)}(\{\lambda p_i\}) = \lambda^{d - N d_\phi + M d_{\phi^2}} \Gamma^{(N,M)}(\{p_i\}) \tag{8.5}$$

where

$$d_\phi = \tfrac{1}{2}(d-2+\eta)$$

is the full scale dimension of ϕ, while

$$d_{\phi^2} = -\nu^{-1}$$

is the full scale dimension of ϕ^2; ν is the critical exponent of the correlation length.

Let us assume that for $p/\Lambda \ll 1$ there exists a scaling limit of $\psi(p)$; then (8.5) with $N=2$, $M=1$, $\eta=(\epsilon/3)$ implies:

$$\psi(p) = B(p/\Lambda)^{d/3-1/\nu}. \tag{8.6}$$

The substitution of this scaling form in equations (8.3) would lead again to a change of the constant term, $Q_0 \to Q_1$. So

$$B(p/\Lambda)^{d/3-1/\nu} = Q_1 + 2C^{*-1}B\Lambda^{1/\nu-d/3}I_\Lambda(p) \tag{8.7}$$

where

$$I_\Lambda(p) = \int_{0<q<\Lambda} \mathrm{d}^d q (\boldsymbol{q}^2)^{-d/6-1/2\nu}[(\boldsymbol{p}-\boldsymbol{q})^2]^{-d/6}. \tag{8.8}$$

The conditions for the ultraviolet and infra-red convergence of the integral $I_\infty(p)$ are,

$$(3/2d) < \mathrm{Re}\ \nu < (3/d). \tag{8.9}$$

Suppose that these conditions are satisfied; in that case we make another transformation of the integral term in the equation and replace $I_\Lambda(p)$ by $I_\infty(p)$. This leads to another change of the constant term of the equation, $Q_1 \to Q$, since

$$\lim_{p\to 0}\{\Lambda^{1/\nu-d/3}[I_\infty(p)-I_\Lambda(p)]\} = (1/\nu - d/3)^{-1}. \tag{8.10}$$

$I_\infty(p)$ can be computed by continuation in the number of dimensions. The result is:

$$2C^{*-1}I_\infty(p) = Dp^{d/3-1/\nu} \tag{8.11}$$

$$D \equiv -2\frac{\Gamma(d/6)\Gamma(2d/3)}{\Gamma(-d/6)\Gamma(d/3)} \cdot \frac{\Gamma(d/3-1/2\nu)\Gamma(1/2\nu-d/6)}{\Gamma(2d/3-1/2\nu)\Gamma(1/2\nu+d/6)}. \tag{8.12}$$

So we are led to the equation:

$$B(p/\Lambda)^{d/3-1/\nu} = Q + DB(p/\Lambda)^{d/3-1/\nu} \tag{8.13}$$

where Q is a constant.

Equation (8.13) must be an identity. Hence

$$D = 1 \tag{8.14}$$

is the equation for ν. The constant B can be determined from the equation $Q=0$. The form of that equation depends on the high momentum behaviour of the two vertex functions. The equation for B is not pursued any further, since it is immaterial to our analysis.

9. Solution of the equation for ν

Equation (8.14), together with (8.12), can be written as:

$$F(x, d) = -2F(0, d), \tag{9.1}$$

with

$$F(x, d) = \frac{\Gamma(x + d/6)\Gamma(2d/3 - x)}{\Gamma(x - d/6)\Gamma(d/3 - x)}, \tag{9.2}$$

and $x = 1/2\nu$. The inequality (8.9) becomes, in terms of x,

$$d/6 < \mathrm{Re}\, x < d/3. \tag{9.3}$$

The first surprise appears already for small values of $\epsilon = 6 - d$. Expanding both sides of equation (9.1) to order ϵ one finds two solutions:

$$x_1 = 1 + 5\epsilon/6 \qquad \nu_1 = \tfrac{1}{2} - 5\epsilon/12 \tag{9.4a}$$

$$x_2 = 2 - 4\epsilon/3 \qquad \nu_2 = \tfrac{1}{4} + \epsilon/6. \tag{9.4b}$$

These correspond to anomalous dimensions of ϕ^2

$$\delta_1 = \nu_1^{-1} - 2 + \eta = 2\epsilon \tag{9.5a}$$

$$\delta_2 = \nu_2^{-1} - 2 + \eta = 2 - 7\epsilon/3 \tag{9.5b}$$

Clearly, it is the first value which is the only one that can be obtained by renormalised perturbation theory. In fact (9.5*a*) is the same as the value obtained in previous studies of the Potts model near six dimensions (Priest and Lubensky 1976, Amit 1976). But the second value—(9.4*b*) or (9.5*b*) is also consistent with all the requirements placed on the variables.

The special feature, apart from the appearance of two values of ν, is that δ_2 does not become small as $\epsilon \to 0$. It tends to the finite value 2. This could never have been reached by perturbation theory.

We return to discuss the implications of these results in the next section. But first we complete the analysis of equation (9.1). The appearance of the two roots becomes natural if one transforms the equation to another variable

$$z \equiv (12/d)x - 3 = (6/d\nu) - 3. \tag{9.6}$$

In terms of z

$$F(x, d) = \frac{\Gamma((5 + z)\delta)\Gamma((5 - z)\delta)}{\Gamma((1 + z)\delta)\Gamma((1 - z)\delta)} \equiv H(z, \delta) \tag{9.7}$$

with $\delta = d/12$. The range of convergence (9.3) is, in terms of z,

$$|\mathrm{Re}\, z| < 1 \tag{9.8}$$

and equation (9.1) becomes

$$H(z, \delta) = -2H(3, \delta). \tag{9.9}$$

The appearance of two roots is a simple consequence of the symmetry of H under $z \to -z$. The values of z corresponding to (9.4) are

$$z_{1,2} = \mp(1 - 2\epsilon). \tag{9.10}$$

In § 6 it was pointed out that $d=3$ is a lower boundary for the present type of calculation. At this value the amplitude of G vanishes, $h=0$, but the 'coupling constant' of equation (8.3) $h^3 w_0^{*2} = 2C^{*-1} \neq 0$ and hence $\psi \neq Q_0$. At $d=3$ equation (9.9) can easily be solved, since

$$F(x, 3) = H(z, \tfrac{1}{4}) = (1-z^2)/16, \tag{9.11a}$$

$$F(0, 3) = H(3, \tfrac{1}{4}) = -\tfrac{1}{2}. \tag{9.11b}$$

Hence

$$z_{1,2} = \pm i\sqrt{15} \tag{9.12}$$

and there is no scaling. The $d=3$ case is considered in detail in Appendix II.

To investigate the range of dimensionalities within which equation (9.9) has real solutions we first note (See Appendix III) that $H(z, \delta)$ is a monotonically decreasing function of z for $0<z<1$. So at the real z axis in the region (9.8) it has its minima at $z=\pm 1$ and a maximum at $z=0$. Hence the values of δ for which real solutions exist are those for which $H(1, \delta) \leqslant -2H(3, \delta) \leqslant H(0, \delta)$. But

$$H(1, \delta) = 0$$

for all δ, while $-2H(3, \delta)$ is positive in the range $\frac{1}{4}<\delta<\frac{1}{2}$, namely, when $3<d<6$. Values of d outside this range are of no interest anyway in the present calculation.

The conclusion from the above consideration is that the condition for a real solution reduces to:

$$H(0, \delta) \geqslant -2H(3, \delta). \tag{9.13}$$

(See in this connection the discussion in the next section.) In figure 12 these two functions are plotted and we find that the inequality (9.13) is satisfied for:

$$0.477 = \delta_0 \leqslant \delta \leqslant 0.5 \tag{9.14a}$$

or

$$5.72 = d_0 \leqslant d < 6. \tag{9.14b}$$

As d approaches the boundary of the region, i.e. $d \to d_0$, $z \to 0$. This is implied simply by the fact that δ_0 is determined by the equality (9.13)

$$-2H(3, \delta_0) = H(0, \delta_0) \tag{9.15}$$

which together with equation (9.9) means that $z(\delta_0) = 0$. In other words, the point at which the real ν disappears is well *within* the range (8.8), which ensures that all our assumptions about the convergence of the integral term of equation (8.7) (which led us to equations (8.13), (8.14)) are valid.

10. Discrimination between the two values of ν

In the previous section we encountered two related problems: the equation for ν (8.14) had two solutions for some dimensions ($d_0 < d < 6$) and no real solution for other values of d ($3 < d < d_0$). In order to discriminate between the two values of ν, for $d > d_0$, we recall that the integral equation (5.17) follows from figure 11 which represents the partially summed perturbation theory series—a series of skeleton graphs.

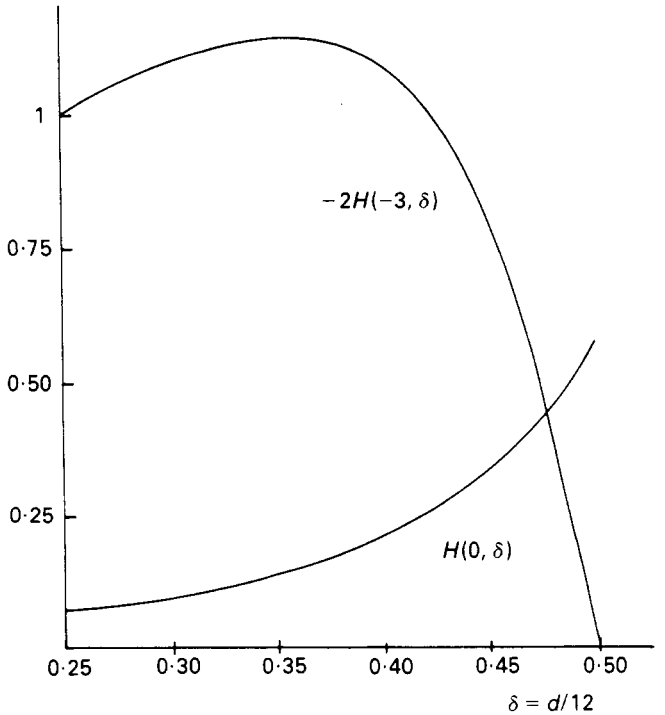

Figure 12. A plot of $H(0, \delta)$ and $-2H(-3, \delta)$ which determines δ_0.

However, the sum of the series of figure 11 is not the only solution of equation (5.17). The existence of another solution is due to the infra-red singularity of its kernel which violates the conditions for the Fredholm uniqueness theorem.

It is this non-uniqueness which causes the existence of the second value of ν. This second value has nothing to do with the series of skeleton graphs of figure 11 and we consider it as alien to the model. In order to be able to judge the relation of ν to the series of skeleton graphs, we must consider its dependence on the coupling constant, but the latter was fixed before arriving at (8.14).

To restore the dependence on the coupling constant we modify temporarily the series of figure 11 (and equation (5.17)), replacing g_0^2 by λg_0^2, λ is an arbitrary coefficient which should be set equal to unity at the end.

The equation (9.9) determining $\nu(\lambda)$ (or $z(\lambda)$) becomes:

$$H(z, \delta) = -2\lambda H(3, \delta) \tag{10.1}$$

The condition (9.13) is, in terms of λ

$$\lambda_0(\delta) \geqslant 1 \tag{10.2}$$

where

$$\lambda_0(\delta) = -[2H(3, \delta)]^{-1} H(0, \delta). \tag{10.3}$$

The modified series of figure 11 reduces to unity at $\lambda = 0$. From equation (8.6) it therefore follows that the acceptable λ dependence of ν must be such that

$$\lim_{\lambda \to 0} \nu(\lambda) = (3/d), \qquad \lim_{\lambda \to 0} z(\lambda) = -1. \tag{10.4}$$

Let us denote this solution by $\nu_+(\lambda)$, $z_+(\lambda)$. There exists a second solution $z_-(\lambda) = -z_+(\lambda)$ at any λ, which tends to $+1$ as $\lambda \to 0$ and which must be rejected. With this in mind, we consider three possible pictures.

(1) If $\lambda_0(\delta) > 1$, then

$$z_+(\lambda) < 0 \qquad z_-(\lambda) > 0 \tag{10.5}$$

for any $0 \leqslant \lambda \leqslant 1$, and the two solutions are separable and identifiable at $\lambda = 1$. This is the case at $d_0 < d < 6$ as is seen from figure 12. In this range of space dimensions the skeleton graph 'perturbation theory' prescribes the choice of solution with vanishing anomalous dimensions as $d \to 6$. Note that $\lambda_0 \to \infty$ as $d \to 6$.

(2) If $\lambda_0(\delta) = 1$ (this is the case at $d = d_0$) then

$$z_+(1) = z_-(1) = 0 \tag{10.6}$$

and there is a single real value of $\nu (\nu = 2/d_0)$.

(3) If $0 < \lambda_0(\delta) < 1$, the two solutions coalesce at $\lambda = \lambda_0 < 1$:

$$z_+(\lambda_0) = z_-(\lambda_0) = 0 \tag{10.7}$$

and are equally acceptable at $\lambda = 1$, or rather, they are equally unacceptable: both of them are complex at $\lambda > \lambda_0$, because $z^2(\lambda)$ changes its sign at $\lambda = \lambda_0$.

To convince oneself one simply notes that

$H(z, \delta)$ is an even function of z and it is $z^2(\lambda)$ which is determined by equation (10.1). Note also that $z^2 = 0$ cannot be a minimal value of z^2, since $\partial z^2/\partial\lambda$ is not zero at $z^2 = 0$ (see Appendix III, equation (AIII.6)).

In figure 12 one sees that the existence of such λ_0 is the case at $d < d_0$. λ_0 is a branch point of $\Gamma^{(2,1)}$, which implies that the series of figure 11 is divergent at $\lambda = 1 > \lambda_0$. Our considerations show that the analytical continuation in λ (with the help of equation (5.17) is not a way out at $d < d_0$.

11. Discussion

Clearly, the model, in the limit of infinite l, is completely soluble. Equations (5.15) and (5.17) can be fully analysed, as well as other relevant quantities. Here we have not embarked on the detailed solution. Instead, we described the model and presented a preliminary study of its asymptotic behaviour. The main purpose being to show that the model is not only soluble, but may contain some surprises as well.

We have found, by studying the infinite l limit of the model, that the two point function scales for d everywhere between 3 and 6. Its temperature derivative scales only in a small subinterval of dimensions (see equation (9.14)). What is more is that in this small range of d the anomalous dimensions of ϕ^2—or the exponent ν—can have two values; one which vanishes as $d \to 6$ the other remaining finite.

The discrimination between the two values is done by considering the solution of the problem in a skeleton expansion. We find that the correlation functions with ϕ^2 insertions develop a branch point at a finite value of the coupling constant—a rather unexpected result.

In fact, the absence of scaling for $d < d_0$ may seem in contradiction with renormalisation group analysis. One usually tends to conclude that all vertex functions scale together, since at the fixed point only constants are left in all the renormalisation group

equations. The function $\Gamma^{(2,1)}$ satisfies the equation:

$$\left[\kappa\frac{\partial}{\partial\kappa}+\beta(u)\frac{\partial}{\partial u}-\gamma_\phi(u)-\gamma_{\phi^2}(u)\right]\Gamma^{(2,1)}(p_1,p_2;p_3;u,\kappa)=0$$

with γ_{ϕ^2} – the anomalous dimension function of the operator ϕ^2. At the point $u=u^*$, at which $\beta=0$, $\Gamma^{(2,1)}$ would seem to scale, just like $\Gamma^{(2)}$.

However, the appearance of a branch point in $\Gamma^{(2,1)}$ entails a branch point in $\gamma_{\phi^2}(u)$. The cut cannot, of course, be detected in perturbation theory.

But, a cut in $\Gamma^{(2,1)}$ implies a cut in $\Gamma^{(2)}$ as a function of temperature (or mass). Away from the critical temperature (as the mass moves away from zero), Z_{ϕ^2} enters in $\Gamma^{(2)}$ as the temperature renormalisation constant, and with it the cut.

This may be a symptom of the general pathological nature of ϕ^3 field theories. Yet it is difficult to conceive of how the addition of a ϕ^4 term may change the situation when a massless theory exists. The solutions found (see equations (6.6), (6.15–17), (8.6), (8.12), (8.14)) demonstrate that massless states are indeed present and thus the ϕ^4 term must be irrelevant. But one must still make sure that at the point of vanishing mass the symmetry is not yet broken.

This requires further analysis, and touches upon the general problem of critical points of systems with ϕ^3 interactions (Priest and Lubensky 1976, Amit 1976).

Acknowledgments

We are grateful to Hadassa Jacobson for her help with numerical computations, and to Drs C Itzykson, E Rabinovici, G Horwitz and I Katznelson for discussions.

Appendix I. Asymptotics of $3nj$-symbols

In this appendix we present the arguments leading to our conclusion that isospin graphs which are not fully two-particle reducible become negligible as $l\to\infty$. In other words, this is our defence of equation (5.4). We do not possess a full proof. Instead we argue as follows:

(A) We show that the $3nj$-symbols of the first and second kind do indeed satisfy (5.3).

(B) Numerical computations of more complex $3nj$-symbols convince us that for the same l and n, the $3nj$-symbols of the first and second kind are uniformly greater than all the other $3nj$-symbols. We present some of these numerical results.

We start with some general considerations:

Any conventional $3nj$-symbol can be represented by a sum

$$(3nj)=\sum_{x_1,\ldots,x_k}(x_1)\ldots(x_k)(6j)_{1,\ldots,}(6j)_N(-)^\psi \tag{AI.1}$$

where $N=n+k-1$, $(x)\equiv 2x+1$.

Wigner (1959) proposed an asymptotic estimate of the $6j$-symbol for large angular momenta:

$$\begin{pmatrix} l_1 & l_2 & l_3\\ l_4 & l_5 & l_6\end{pmatrix}\sim\begin{cases}\dfrac{1}{\sqrt{24\pi V}} & V^2>0\\ 0 & V^2<0\end{cases} \tag{AI.2}$$

where V is the volume of the tetrahedron with edges $\lambda_i = l_i + \frac{1}{2}$, $i = 1, \ldots, 6$, given by:

$$2^5 3^2 V^2 = \begin{vmatrix} 0 & \lambda_4^2 & \lambda_5^2 & \lambda_6^2 & 1 \\ \lambda_4^2 & 0 & \lambda_3^2 & \lambda_2^2 & 1 \\ \lambda_5^2 & \lambda_3^2 & 0 & \lambda_1^2 & 1 \\ \lambda_6^2 & \lambda_2^2 & \lambda_1^2 & 0 & 1 \\ 1 & 1 & 1 & 1 & 0 \end{vmatrix} \equiv 2J(\{\lambda_i\}). \tag{AI.3}$$

In fact the $6j$-symbol is a rapidly oscillating function of its indices at $V^2 > 0$ and is damped by an exponentially decreasing factor at $V^2 < 0$:

$$\begin{Bmatrix} l_1 & l_2 & l_3 \\ l_4 & l_5 & l_6 \end{Bmatrix} \simeq \frac{1}{\sqrt{12\pi|V|}} C. \tag{AI.4}$$

The function C was found by Ponzano and Regge (1968); the average of C^2 over several contiguous values of l_i at $V^2 > 0$ is $\frac{1}{2}$. Equation (AI.4) is an excellent asymptotic approximation for the $6j$-symbol which turns out to be satisfactorily accurate even for small values of $\{l_i\}$. But it is certainly inaccurate in the neighbourhood of the point $V = 0$.

An asymptotic formula, which is correct in the transitional region $V \simeq 0$, was given by Ponzano and Regge (1968):

$$\begin{Bmatrix} l_1 & l_2 & l_3 \\ l_4 & l_5 & l_6 \end{Bmatrix} \simeq (-)^{\Phi} 2^{-4/3} \Big(\prod_{h=1}^{4} A_h \Big)^{-1/6} \mathrm{Ai}\Big[-\frac{(3V)^2}{(4\prod_{h=1}^{4})^{2/3}} \Big]; \tag{AI.5}$$

here A_h, $h = 1, \ldots, 4$ are the areas of the faces of the tetrahedron, $\mathrm{Ai}(z)$ is the Airy function.

We simplify the analysis using Wigner's estimate (AI.2) everywhere except in the transitional region, where we approximate the $6j$-symbol by a constant, which is the value of equation (AI.5) at the point $V = 0$.

We insert this approximation in equation (AI.1) and suppress all oscillations—those present in the $6j$ symbols as well as the explicit ones ($(-1)^{\Psi}$) in equation (AI.1). This way we majorise the sum. The application of Wigner's estimate neglects that part of the sum (AI.1) in which $V_j^2 < 0$. This part cannot influence the asymptotic behaviour of the sum since the $6j$-symbols decrease very rapidly in this region.

In terms of the variables

$$\lambda = l + \tfrac{1}{2} \tag{AI.6}$$

$$\xi_i = \frac{x_i + \frac{1}{2}}{2\lambda} \qquad \xi_i = \frac{1}{4\lambda}, \frac{3}{4\lambda}, \frac{5}{4\lambda}, \ldots, \tag{AI.7}$$

Wigner's formula (AI.2) for a $6j$-symbol, entering equation (AI.1), takes the form

$$(6j) \simeq (2\pi)^{-1/2} \lambda^{-3/2} \tilde{J}^{-1/4}, \tag{AI.8}$$

where

$$\tilde{J} \equiv J|_{\lambda = 1}$$

is a function of ξ_i only.

The value of the $6j$-symbol at the transitional point $V = 0$ is, according to equation (AI.5),

$$|(6j)| \simeq 2^{-4/3} 3^{-2/3} (\Gamma(\tfrac{2}{3}))^{-1} \Big(\prod_{h=1}^{4} A_h \Big)^{-1/6} \Big|_{V=0}. \tag{AI.9}$$

We denote the 'width' of the transitional region by v. This is some small value of the volume of the tetrahedron. Approximating the $6j$-symbol by equation (AI.8) for $V > v$ and by equation (AI.9) for $0 < V < v$ leads to the expression

$$|(3nj)| \simeq \text{const} \times \lambda^{1/2(-3n+k+3)} \int_{(4\lambda)^{-1}} \cdots \int_{(4\lambda)^{-1}} \prod_{i=1}^{k} \xi_i \, d\xi_i \prod_{j=1}^{n+k-1} \tilde{J}_j^{-1/4} \, \theta(V_j - v_j) + T_n(\lambda) \tag{AI.10}$$

where $T_n(\lambda)$ is the contribution of the terms in which some of the V_j's are in the transitional region $V_j^2 < v_j^2$.

(i) Consider first the $3nj$-symbols of the first and second kind, when in equation (AI.1) there is a single sum ($k = 1$), as well as a single integral in equation (AI.10).

All the n $6j$-symbols in equation (AI.1) ($N = n$ in this case) are identical (recall that all the $3n$ angular momenta of the $3nj$-symbol considered are equal to l). Equation (AI.10) obtains the form:

$$|(3nj)_{1,2}| \simeq \text{const} \, . \, \lambda^{-3n/2+2} \int_{(4\lambda)^{-1}}^{\xi_0 - \Delta\xi} d\xi \cdot \xi [\tilde{J}(\xi)]^{-n/4} + T_n(\lambda) \tag{AI.11}$$

with

$$\tilde{J}(\xi) = 4\xi^2(3 - 4\xi^2) \equiv 16\xi^2(\xi_0^2 - \xi^2) \tag{AI.12}$$

$$\xi_0 = (\sqrt{3}/2) \qquad V(\xi_0) = 0 \tag{AI.13}$$

When $V = 0$, all the four areas A_h are identical and equal to $3^{1/2} \, 2^{-2} \, \lambda^2$; thus the value of the $6j$-symbol at that point is, according to equation (AI.9),

$$|6j(\xi_0)| \simeq [3\Gamma(2/3)]^{-1} \lambda^{-4/3}. \tag{AI.14}$$

The boundary of the transitional region can be naturally defined as that value of $\xi = \xi_0 - \Delta\xi$ for which Wigner's expression (AI.8) obtains the value (AI.14). It turns out to be

$$\Delta\xi \sim \lambda^{-2/3}. \tag{AI.15}$$

So the term $T_n(\lambda)$ of equation (AI.11) is

$$T_n(\lambda) = \text{const} \, . \, \lambda^2 \, . \, \lambda^{-2/3} \, . \, \lambda^{-4n/3} = \text{const} \, . \, \lambda^{-4n/3+4/3}. \tag{AI.16}$$

The integral in equation (AI.11) can be represented as

$$I((4\lambda)^{-1}, \xi_0 - \Delta\xi) \equiv I((4\lambda)^{-1}, \xi_1) + I(\xi_1, \xi_2) + I(\xi_2, \xi_0 - \Delta\xi) \tag{AI.17}$$

where

$$\xi_1 \ll 1 \qquad \xi_0 - \Delta\xi - \xi_2 \ll 1$$

are λ independent small numbers, so that

$$\mathrm{I}((4\lambda)^{-1}, \xi_1) \sim \int_{(4\lambda)^{-1}}^{\xi_1} d\xi \, . \, \xi \, . \, \xi^{-n/2} \sim \lambda^{n/2-2} \tag{AI.18}$$

$$I(\xi_2, \xi_0 - \Delta\xi) \sim \int_{\xi_2}^{\xi_0 - \Delta\xi} d\xi (\xi_0 - \xi)^{-n/4} \sim (\Delta\xi)^{-n/4+1} \sim \lambda^{n/6-2/3} \tag{AI.19}$$

while $I(\xi_1, \xi_2)$ is finite. Thus the term $\lambda^{-3n/2+2} I(\xi_2, \xi_0 - \Delta\xi)$ is of the same order as $T_n(\lambda)$ (equation (AI.16)) and equation (AI.11) becomes

$$|(3nj)_{1,2}| \leqslant C_1\lambda^{-n} + C_2\lambda^{-3n/2+2} + C_3\lambda^{-4n/3+4/3}. \tag{AI.20}$$

In equation (AI.20) the first ('infrared') term dominates for $n \geqslant 4$, which gives $\alpha = 1$ in equation (5.3). For $n = 3$ the dominant term is the second one; that is, the $9j$-symbol falls off as $\lambda^{-5/2}$ (or faster), implying $\alpha = 1/2$.

(ii) For $n > 4$ there are more than two kinds of $3nj$-symbols. The $3nj$ symbols of the kinds other than the first or second one are given by multiple sums ($k > 1$ in equation (AI.1)), which complicates the analysis. Proceedings as in equation (AI.17) and using equation (AI.10) we see that the 'middle part' of the integral (the analogue of $I(\xi_1, \xi_2)$) contributes

$$\lambda^{(-3n+k+3)/2} \tag{AI.21}$$

which implies $\alpha = (n - k - 1)/2$.

It can be shown, that any $3nj$-symbol may be represented by equation (AI.1) with $k \leqslant n - 2$, which provides (for the contribution of this term) $\alpha \geqslant 1/2$. But this inequality for k depends on the representation of the $3nj$-symbol. In fact, in some of the commonly used formula it does not hold. The graph of the $3nj$-symbol can be transformed to obtain different representations of that symbol in terms of lower ones (with less indices). The common representation leads to an expression in terms of the simplest lower $3nj$-symbols. But this does not necessarily provide the lowest value for k in equation (AI.1).

For example, the $15j$-symbol of the 5th kind is commonly represented as

$$(15j)_5 = \Sigma(x_1)(x_2)(-)^{\psi} 6j(x_1)6j(x_2)[9j(x_1, x_2)]^2 \tag{AI.22}$$

which leads to equation (AI.1) with $k = 4$, if we express the $9j$-symbol in terms of the $6j$-symbols. But it can be represented as

$$(15j)_5 = \Sigma(x_1)(x_2)(-)^{\phi} 6j(x_1)6j(x_2)6j(x_1, x_2)12j(x_1, x_2) \tag{AI.23}$$

which implies $k = 3$. Equation (AI.23) is obtained with the help of the graphical decomposition, shown in figure 13 and by using the identity of figure 7 for the '3-particle reducible' closed isospin graph.

The other parts of the multiple integral in equation (AI.10) have not been considered in the general case. Consideration of the $15j$- and $18j$-symbols raises a hope that the contribution of the transitional region does not dominate and that the 'infrared' behaviour is not too singular, so that the inequality $\alpha > 0$ always holds.

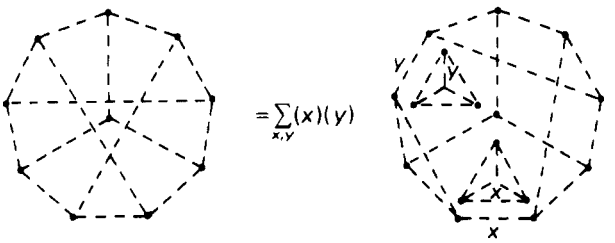

Figure 13. The graphical decomposition of the $15j$-symbol of the 5th kind.

$3nj$-symbols of different kinds have been computed for $n \leqslant 8$ for many values of l. Samples of $15j$- and $18j$-symbols are plotted in figure 14. In every case we plot the ratio of the computed conventional $3nj$-symbol divided by $(2l+1)^{-(n-1)}$—the trivial $3nj$-symbol, represented by a fully 2PR graph, equation (5.1). For comparison we plot also the same ratio with the estimate (5.3) for the $3nj$-symbol, if $\alpha = 1/2$; i.e. $(2l+1)^{-1/2}$.

Without exception, for all values of l, the $3nj$-symbols of the first and second kind are greater than the others for the same values of n and l.

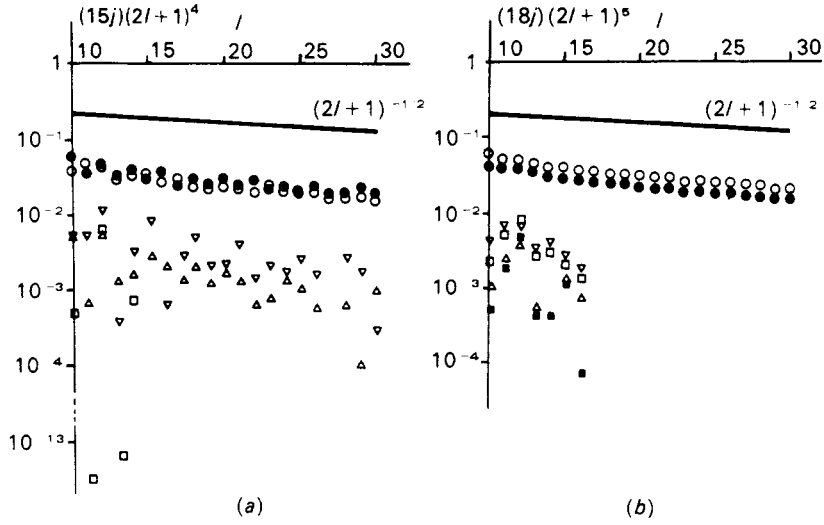

Figure 14. The $15j$-symbols and a few kinds of the $18j$-symbols compared with the fully 2PR graphs. $|(3nj)|(2l+1)^{n-1}$ are plotted, together with $(2l+1)^{-1/2}$, which would have been the line if α were $\frac{1}{2}$. The numbers which correspond to the kinds of $15j$- and $18j$-symbols are as follows. In (*a*): ●, 1; ○, 2; △, 3; ▽, 4; ■, 5 and (*b*): ●, 1; ○, 2; △, 4; ▽, 7; ■, 11; □, 18.

Appendix II. Solution in three dimensions

From equations (6.16) and (6.19) it follows that $d = 3$ is a pole of the function $w_0^{*2}(d)$. On the other hand $h(d) = 0$ at $d = 3$ (equation (6.17)), so the expression (6.6) for $G(p)$ vanishes at $d = 3$.

But if we consider equation (6.5) at $d \neq 3$ with $w_0 = w_0^*(d)$ and insert into it

$$G(p) = h\Lambda^{-\epsilon/3} p^{-d/3} \tag{AII.1}$$

with $h = h(d)$, we find that equation (6.5) is exactly satisfied in the limit $d \to 3$.

Inserting equation (AII.1) into equation (5.17) and performing the limit $d \to 3$ we come to an integral equation

$$\psi(\boldsymbol{r}, \boldsymbol{a}) = 1 + \frac{1}{\pi} \int \mathrm{d}^d r' \frac{\psi(\boldsymbol{r}', \boldsymbol{a})}{|\boldsymbol{r} - \boldsymbol{r}'|\,|\boldsymbol{a} - \boldsymbol{r}'|\,|\boldsymbol{a} + \boldsymbol{r}'|} \tag{AII.2}$$

with

$$\psi(\boldsymbol{r}, \boldsymbol{a}) \equiv \Gamma^{(2,1)}(\boldsymbol{p}_1, \boldsymbol{p}_2), \qquad \boldsymbol{r} = \tfrac{1}{2}(\boldsymbol{p}_1 - \boldsymbol{p}_2), \qquad \boldsymbol{a} = \tfrac{1}{2}(\boldsymbol{p}_1 + \boldsymbol{p}_2). \tag{AII.3}$$

Equation (AII.2) is an integral form of the Schrodinger equation

$$\frac{\hbar^2}{2m}\Delta\psi - U(\boldsymbol{r})\psi = 0, \qquad U(\boldsymbol{r}) = -\frac{2\hbar^2}{m}\frac{1}{|\boldsymbol{a}-\boldsymbol{r}|\,|\boldsymbol{a}+\boldsymbol{r}|} \tag{AII.4}$$

for the zero energy stationary state of a particle moving in the potential field $U(\boldsymbol{r})$.

We do not pursue equations (AII.2), (AII.4) any further at a nonvanishing value of $\boldsymbol{a}$ and return to the function $\psi(p)$(equation (8.2)) at $\boldsymbol{p}_1 = -\boldsymbol{p}_2 = \boldsymbol{p}$. When $\boldsymbol{a} = 0$, equation (AII.4) coincides with the equation considered in § 35 of Landau and Lifshitz (1959). The integral equation (AII.2) implies that $\psi(\boldsymbol{r})$ must be spherically symmetric; thus the 'angular momentum' $l = 0$.

In the notation of Landau and Lifshitz (1959)

$$\beta = (2\hbar^2/m) \qquad \gamma = 4 \qquad s_{1,2} = -\tfrac{1}{2} \pm (\mathrm{i}/2)\sqrt{15}. \tag{AII.5}$$

The contact with the notation of §§ 8, 9 (see e.g. equations (8.6), (9.6) is:

$$s_{1,2} = -\tfrac{1}{2}(1 + z_\pm) \tag{AII.6}$$

and thus:

$$z_\pm = \mp \mathrm{i}\sqrt{15}. \tag{AII.7}$$

If we modify equations (AII.2), (AII.4), introducing the 'coupling constant' λ, as in § 10, equation (AII.7) changes to

$$z_\pm = \mp\sqrt{1 - 16\lambda}. \tag{AII.8}$$

λ_0 of § 10 is now equal to 1/16. It is the branch point of the function $z(\lambda) = \sqrt{1-16\lambda}$. $z_\pm(\lambda)$ are the two branches of this function.

The general solution of equation (AII.4) is

$$\psi(r) = r^{-1/2}(B_+ r^{-z_+/2} + B_- r^{-z_-/2}). \tag{AII.9}$$

The requirement, $\psi(r) = 1$ at $\lambda = 0$, chooses the solution with $B_- = 0$ at $\lambda < 1/16$, but it fails to distinguish between the two branches $z_\pm$ at $\lambda > 1/16$. Equation (AII.9) at $\lambda = 1$ can be rewritten as

$$\psi(r) = \left[\frac{r_0}{r}\right]^{1/2} \cos\left(\frac{\sqrt{15}}{2}\ln\frac{r}{r_1}\right) \tag{AII.10}$$

with constant r_0 and r_1. No choice of these constants can provide scaling.

Appendix III. Some properties of the function H

It follows from the definition of $H(z, \delta)$ (equation (9.7)) that

$$(\partial H/\partial z) = H\delta\{\psi((5+z)\delta) - \psi((5-z)\delta) - \psi((1+z)\delta) + \psi((1-z)\delta)\} \tag{AIII.1}$$

where

$$\psi(z) = \frac{\mathrm{d}}{\mathrm{d}z}\ln\Gamma(z) = -\gamma - \frac{1}{z} + \sum_{k=1}^{\infty}\left(\frac{1}{k} - \frac{1}{z+k}\right) \tag{AIII.2}$$

So

$$\frac{\partial H}{\partial z^2} = -8\delta^3 H \sum_{k=0}^{\infty}\frac{3\delta + k}{[(5\delta+k)^2 - z^2\delta^2][(\delta+k)^2 - z^2\delta^2]} \tag{AIII.3}$$

and

$$\frac{\partial H}{\partial z^2} < 0 \tag{AIII.4}$$

for $z^2 < 1$.

Equation (10.1) implies that

$$\frac{1}{\lambda}\frac{\partial \lambda}{\partial z^2} = \frac{1}{H}\frac{\partial H}{\partial z^2}. \tag{AIII.5}$$

Thus

$$\left.\frac{\partial \lambda}{\partial z^2}\right|_{z=0} = -8\delta^3 \lambda_0 \sum_{k=0}^{\infty} \frac{3\delta + k}{(5\delta + k)^2(\delta + k)^2} \tag{AIII.6}$$

is finite.

References

Amit D J 1976 *J. Phys. A: Math. Gen.* **9** 1441

Amit D J and DeDominicis C T 1973 *Phys. Lett.* **45A** 193

Amit D J and Scherbakov A 1974 *J. Phys. C: Solid St. Phys.* **7** L96

Amit D J and Zannetti M 1974 *J. Stat. Phys.* **11** 133

Amit D J, Wallace D J and Zia R K P 1977 *Phys. Rev.* B**15** 4657

Ashkin J and Teller E 1943 *Phys. Rev.* **64** 178

Berlin T H and Kac M 1952 *Phys. Rev.* **86** 821

Brezin E, LeGuillou J C and Zinn-Justin J 1976 *Phase Transitions and Critical Phenomena* Vol VI ed C Domb and M S Green (New York: Academic Press)

Brezin E and Zinn-Justin J 1976 *Phys. Rev.* B**14** 3110

Coleman S, Jackiw R and Politzer H D 1974 *Phys. Rev.* D**10** 2491

Dolan L and Jackiw R 1974 *Phys. Rev.* D**9** 3320

Edmonds A K 1957 *Angular Momentum in Quantum Mechanics* (Princeton: Princeton University Press)

Fano V and Racah G 1959 *Irreducible Tensorial Sets* (New York: Academic Press)

Golner G R 1973 *Phys. Rev.* A**8** 3419

t' Hooft G and Veltman H 1972 *Nucl. Phys.* B**44** 189

Jucys A P, Levinson J B and Vanagas V V 1960 *Matematicheski Apparat Teorii Momenta Kolichestva Dvizhenia* (Vilnius 1960) (in Russian); English translation: Yutsis A P, Levinson I B and Vanagas V V *The Mathematical Apparatus of the Theory of Angular Momentum* (Jerusalem 1962)

Jucys A P and Bandzaitis A A 1965 *Teoria Momenta Kolichestva Dvizhenia v Kvantovoi Mekhanike* (Vilnius)

Judd B 1963 *Operator Techniques in Atomic Spectroscopy* (New York: McGraw-Hill)

Kac M and Thompson C J 1971 *Proc. Norwegian Academy of Sciences* **5** 163

Landau L D and Lifshitz E M 1959 *Quantum Mechanics* (London: Pergamon)

Levinson I B 1957 *Trudy Phys. Techn. Instituta A N Litovskoi S S R* **2** 17, 31

Ma S K 1972 *Phys. Rev. Lett* **29** 1311

—— 1973 *Rev. Mod. Phys.* **45** 589

Patashinski and Pokrovski 1964

Ponzano G and Regge T 1968 *Semiclassical Limit of Racah Coefficients, in 'Spectroscopic and Group Theoretical Methods in Physics,'* Racah Memorial Volume (Amsterdam: North-Holland)

Potts R B 1952 *Proc. Camb. Phil. Soc.* **48** 106

Priest R G and Lubensky T C 1976 *Phys. Rev.* B**13** 4159

Schnitzer H J 1974 *Phys. Rev.* D**10** 1800 and 2042

Stanley E H 1971 *Introduction to Phase Transitions and Critical Phenomena* (Oxford: Clarendon Press)

Wigner E P 1959 *Group Theory* (New York: Academic Press)

Wilson K G 1973 *Phys. Rev.* D**7**

Zannetti M and DiCastro C, 1977 *J. Phys. A: Math. Gen.* **10** 1175

Zia R K P and Wallace D J *J. Phys. A: Math. Gen.* **8** 1495